
ELSEVIER
Volume 47
www.elsevier.com
Number 2
February 2010
ISSN 1365-1609
New developments and case studies in rock mechanics and rock engineering
International Journal of
Rock Mechanics and Mining Sciences
Editor-in-Chief: R. W. Zimmerman, Imperial College, London , UK
Unaltered Äspö Diorite
Shear zone
Feldspar plane
Epidote + chlorite filled fracture
Pegmatite
Horizontal cut
Pillar centre
Fracture induced during de-stressing
Mafic inclusion
• fundamental rock behaviour
• in situ stress
• site investigation
• rock cutting and drilling
• underground excavations
• rock reinforcement and support
• dam engineering
• geothermal energy
• petroleum engineering
• radioactive waste disposal
Available online at www.sciencedirect.com
ScienceDirect

International Journal of Rock Mechanics & Mining Sciences 47 (2010) 279–285

Contents lists available at ScienceDirect

International Journal of
Rock Mechanics & Mining Sciences

journal homepage: www.elsevier.com/locate/ijrmms

Investigation of damage-induced permeability of Opalinus clay

M. Jobmann [a,*], Th. Wilsnack [b], H.-D. Voigt [c]

[a] DBE TECHNOLOGY GmbH, Eschenstraße 55, D-31224 Peine, Germany
[b] IBeWa Ingenieurpartnerschaft, Lessingstraße 46, D-09599 Freiberg/Sachsen, Germany
[c] Freiberg University of Mining and Technology, Department of Drilling Engineering and Fluid Mining, Agricolastraße 22, D-09599 Freiberg/Sachsen, Germany

A R T I C L E I N F O

Article history:
Received 25 March 2009
Received in revised form
20 October 2009
Accepted 30 November 2009
Available online 23 December 2009

Keywords:
Damage
Permeability
Opalinus clay
Crack
Effective porosity

A B S T R A C T

An excavation damaged zone (EDZ) around emplacement boreholes for radioactive waste represents a potential pathway for radionuclides due to its increased porosity and crack permeability. As clay is one of the potential host rocks for radioactive waste disposal, Opalinus clay samples from the underground rock laboratory at Mont Terri were investigated regarding their hydraulic properties – and related crack occurrence – after excavation and during stress-dependent crack closure. After determination of their hydraulic properties in untreated conditions, the samples were artificially cracked by tensile strength tests. The cracked samples were put into a triaxial pressure cell and the permeability and effective porosity were measured during stepwise increase and decrease of confining pressure. When the pressure was increased, a continuous decrease of permeability was found, which was similar for all test samples, and a mathematical expression was identified. When the pressure was decreased, no increase of permeability was observed until the samples were completely depressurized, leading to the assumption that during pressurization some kind of sealing process took place resulting in a permanent crack closure. In addition to the dependence on pressure, a time-dependent permeability reduction and thus crack closure at constant pressure was found, indicating a creep compaction behaviour of the clay. By knowing the initial permeability immediately after excavation of an emplacement borehole, the permeability reduction due to time-dependent stress variation can be calculated for use in long-term safety analyses.

1. Introduction

The hydro-mechanical behaviour of clay as a host rock for a repository for radioactive waste has been investigated. According to previous conceptual design studies, the waste disposal in vertical emplacement boreholes is the preferred disposal concept [1,2]. One issue regarding borehole disposal is that due to the drilling and the associated disturbance and damage in the area surrounding the emplacement boreholes: the favourable properties of clay formations could change and the rock could lose part of its barrier function. Stress redistribution will lead to the creation of a so-called excavation damaged zone (EDZ) depending on the initial stress field, the material properties, the existence of natural fracture zones or local inhomogeneities of the rock mass and the geometry of the boreholes. Immediately after excavation, an EDZ consisting of cracks and fissures occurs around the borehole. An EDZ represents a potential pathway for radionuclides due to its increased porosity and crack permeability. A key question to be answered within a safety analysis is how the EDZ around an emplacement borehole evolves as a function of time and stress, respectively, especially with regard to its permeability. A major issue in this context is the considerable amount of heat which, due to radioactive decay, dissipates into the host rock inducing thermal stresses and possibly temperature enhanced creep of the host rock. The latter may lead to a (self-) sealing of the excavation-induced cracks and fissures [3,4]. In the framework of the SELFRAC project sealing and healing mainly of the plastic Boom clay and partly to Opalinus clay was investigated resulting in a rather fast sealing (but not healing) of the Boom clay was found and a much slower sealing of Opalinus clay [5]. Davy et al. [6] investigated the permeability of macro-cracked argillite and found that in case of water being the flowing liquid, a swelling of clay particle led to an additional sealing of fractures. Dedecker et al. proposed a calculation method for hydraulic properties of cracked Callovo–Oxfordian clay using two coupled finite difference computer codes [7].

An important task is to evaluate the thermo-mechanical impact of a filled and thus heated emplacement field on individual boreholes and their EDZ, especially on open emplacement boreholes being prepared to take up new waste canisters [8]. In this paper laboratory investigations are presented describing the permeability and effective porosity, i.e. the pore space

* Corresponding author. Tel. +49 5171431530; fax: +49 5171431506.
E-mail addresses: jobmann@dbe.de, michael.jobmann@gmx.de (M. Jobmann).

1365-1609/$ - see front matter © 2009 Elsevier Ltd. All rights reserved.
doi:10.1016/j.ijrmms.2009.11.009

relevant to fluid flow, of cracked Opalinus clay samples as a function of confining pressure simulating the closing of EDZ cracks by creep behaviour of a clay host rock.

2. Material and methods

The investigated Opalinus clay samples came from the Mont Terri rock laboratory in Switzerland. The depth level is approximately 200 m below surface level. The samples were taken from borehole BHE-D25 drilled in the side wall of a gallery called MI-niche, at a borehole depth range 5–6 m. The horizontal borehole cuts the natural bedding of the clay at an angle of ca. 45°. The obtained drill core samples were packed in suitable plastic tubes directly after drilling. In order to protect them against mechanical damage and extensive drying, the annulus between the tube and the drill core was filled with epoxy resin (Fig. 1). Nevertheless, an influence from drilling and stress relaxation cannot be excluded. The investigations were carried out according to the following steps: (i) preparation of samples from the different drill cores of Opalinus clay, (ii) determination of the initial gas permeability and effective porosity, (iii) artificial damage of the samples by tensile strength tests, and (iv) determination of permeability and effective porosity along drill core axis (45° to bedding) of the cracked samples for different restraint conditions.

2.1. Artificial damage—methodology and application

In preparation for the permeability tests, cylindrical samples with a diameter of 50 and 100 mm were drilled out of the available cores. The orientation of the samples in relation to the bedding of the clay is shown exemplarily for samples D25-3 and D25-4 in Fig. 1. The 100 mm samples from the cores D25-1 and D25-7 were taken with the same orientation as D25-3, which is parallel to the core axis.

For the generation of cracks in the sample a test method called indirect tensile stress test for rock samples—Brazilian test was applied. The test was developed by the German Society for Earth Work and Soil Engineering for the use in rock mechanics. Fig. 2 shows a sketch of the test configuration and the stress distribution over a test sample. The tensile strength σ_t [N] can be determined by [9]

$$\sigma_t = 0.636\,F/dL \qquad (1)$$

where F is the force applied in [N], d the diameter and L the length of the sample, both in [mm]. The test requires samples with a diameter of ≥ 50 mm and a length to diameter ratio of approximately 1. During the tests, the samples were not completely damaged but the load was continuously increased and stopped immediately after cracking. Thus, the cylindrical shape was kept for the subsequent permeability and porosity tests. This kind of test was applied in order to artificially create cracks with increased permeability in the samples (Figs. 3 and 4).

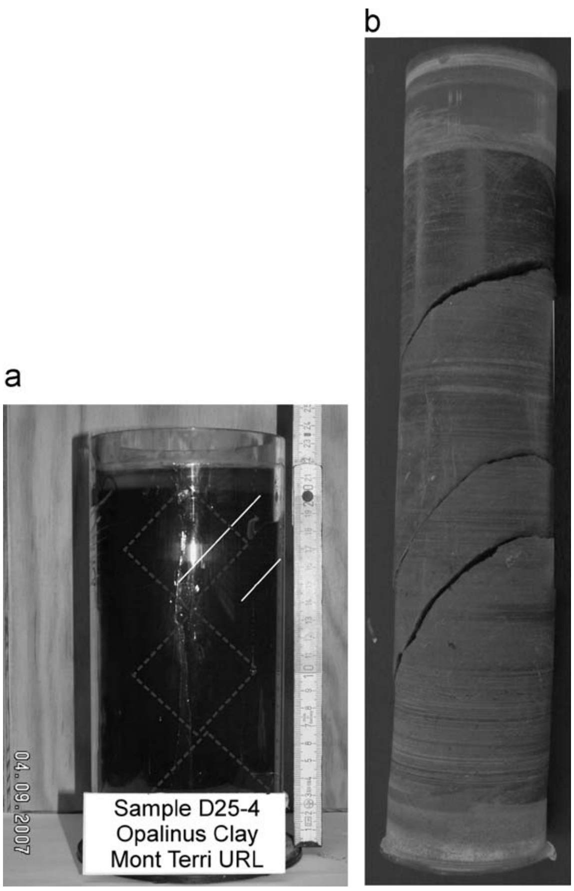

Fig. 1. Core samples of the Opalinus clay: (a) sample D25-4 before drilling including orientation and (b) drilled core sample D25-3 with cracking along the natural bedding.

2.2. Determination of permeability and effective porosity

The determination of permeability is conventionally based on the measurement of a steady state flow process under constant test conditions. The steady state requirement leads to a high experimental effort for the measurement of low flow rates and the keeping of constant test conditions over long test durations, especially for specimens of very low permeability. Therefore, a test concept based on the monitoring of an impulse-induced unsteady flow process was applied for the determination of the permeability of the Opalinus clay [10]. This test configuration is schematically shown in Fig. 5.

The sample is installed in a pressure cell completely covered by a rubber seal. An inflow and outflow gas pressure chamber are connected to the test cell, both having a known volume. The inflow chamber is adjusted to a defined gas pressure and the outflow chamber is adjusted to atmospheric pressure. Both chambers are opened at the same time and the pressure development in both chambers resulting from pressure compensation through the sample are recorded. The knowledge of the

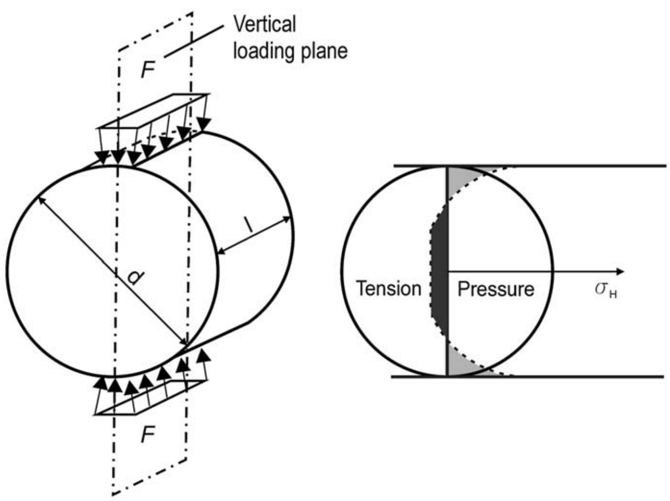

Fig. 2. Sketch of the test configuration and the stress distribution over the sample [6].

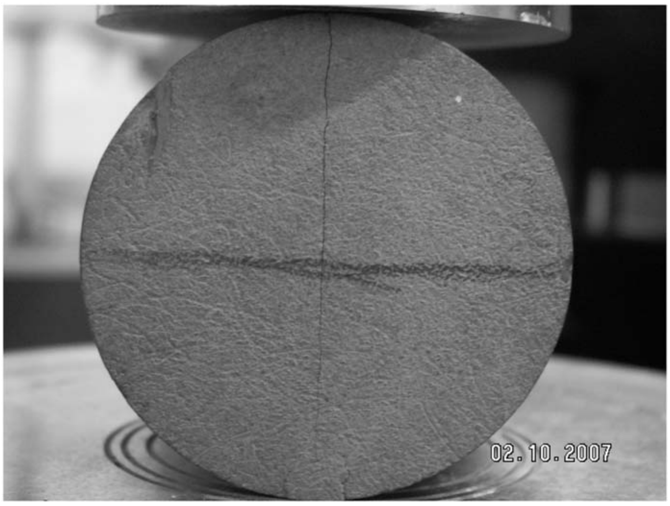

Fig. 3. Cracked sample.

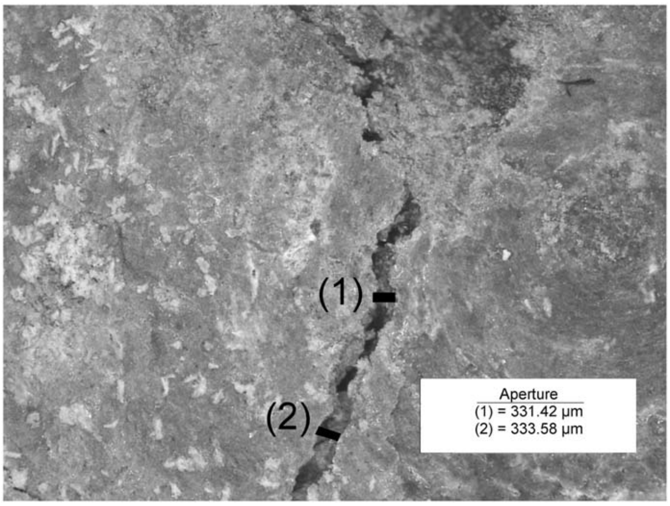

Fig. 4. Crack of sample D25-1.1.

exact volumes of the test equipment (inflow and outflow chamber, sample, lines), the viscosity and compressibility of the fluid, the compressibility of the test equipment and the time-dependent pressure evolution measured in the input and output chamber are essential for the determination of the permeability and the effective porosity. Taking these data into consideration, a numerical model of the flow process was generated for each test to calculate the two time-dependent pressure curves. The identification of permeability and effective porosity was performed by fitting the measured and calculated pressure curves. A fitting of measured data is shown in Fig. 6.

The test method allows the identification of the samples' permeability for gases and liquids in the permeability range between 1×10^{-12} and $1\times10^{-24}\,m^2$, and of the effective porosity down to 0.1%. The main features of the applied test method are the short test duration for very low gas and liquid permeabilities (hours to days) and the simultaneous determination of the permeability and effective porosity.

The permeability investigations on the Opalinus clay samples were done by applying a confining pressure (p_c) from 0.25 to 5.0 MPa. Dry nitrogen was used with a gas injection pressure varying from p_t=$p_c-0.2$ to $p_c-0.3$ MPa. It has to be pointed out that the test method describes a flow process through a partly

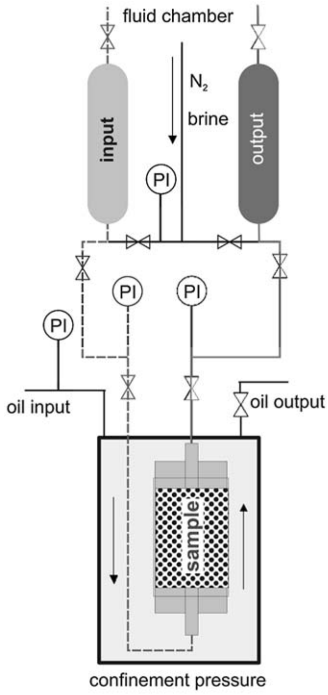

Fig. 5. Schematic diagram of the test configuration.

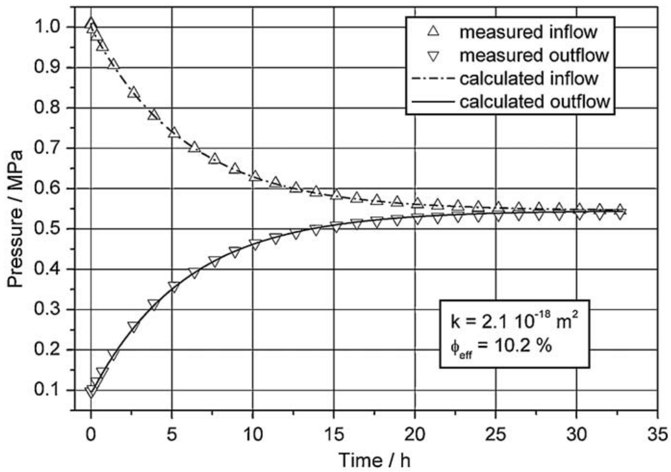

Fig. 6. Measured and calculated pressure curves for permeability and effective porosity identification.

saturated porous medium. Due to these two-phase flow conditions, the determined gas permeability represents the potential flow process and thus should be taken as effective gas permeability.

3. Results and discussion

3.1. *Initial properties*

Prior to cracking the samples several initial properties were determined in order to get information on the untreated situation. Besides permeability, the total and effective porosity as well as the water content and water saturation of each sample was determined. Table 1 gives an overview of sample properties.

The total porosity was determined by using the densities. All initial values are shown in Fig. 7. The initial water content (wt%)

Table 1
Initial properties of samples.

Sample	Length (mm)	Diameter (mm)	Direction of measurement	Density (wet) ($g\,cm^{-3}$)	Mass (wet) (g)	Grain density ($g\,cm^{-3}$)	Initial total porosity (%)	Initial water content (wt. %)	Initial saturation (Vol%)	Tensile strength (MPa)
D25-1.1	27.6	38.6	Axial	2.343	75.69	2.60	12.6	3.1	57	1.09
D25-3.1	28.8	49.4	Axial	2.378	131.23	2.60	10.7	2.4	52	1.80
D25-3.2	27.2	49.4	Axial	2.356	122.74	2.60	11.5	2.4	48	2.49
D25-3.3	27.4	49.4	Axial	2.343	122.95	2.60	12.0	2.4	46	2.02
D25-4.1	51.5	49.4	Axial	2.454	242.25	2.60	6.9	1.4	50	2.13
D25-4.2	50.4	49.5	Axial	2.329	225.90	2.60	11.7	1.4	28	–
D25-7.1	100.0	92.5	Axial	2.372[a]	1672.26	2.60	10.6	2.0	44	1.30

[a] Determined by average of the dry density.

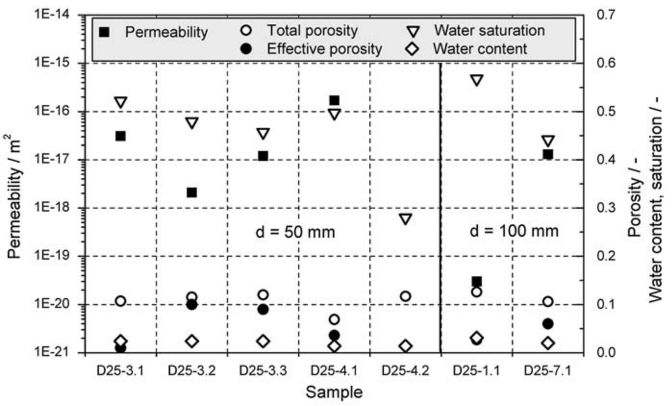

Fig. 7. Initial hydraulic properties of the test samples.

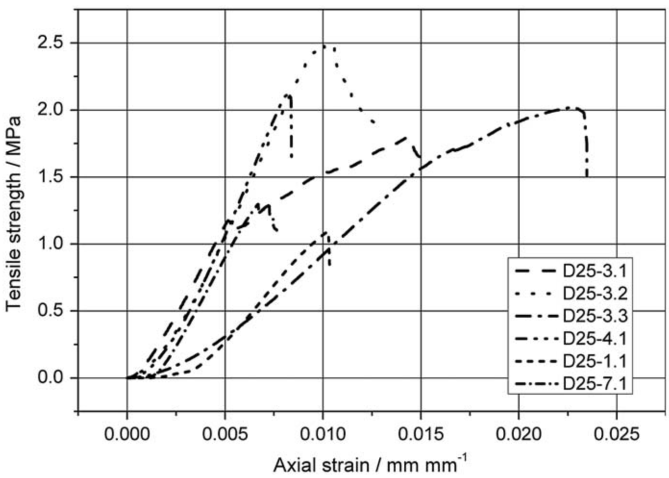

Fig. 8. Strength–strain diagram of the test samples.

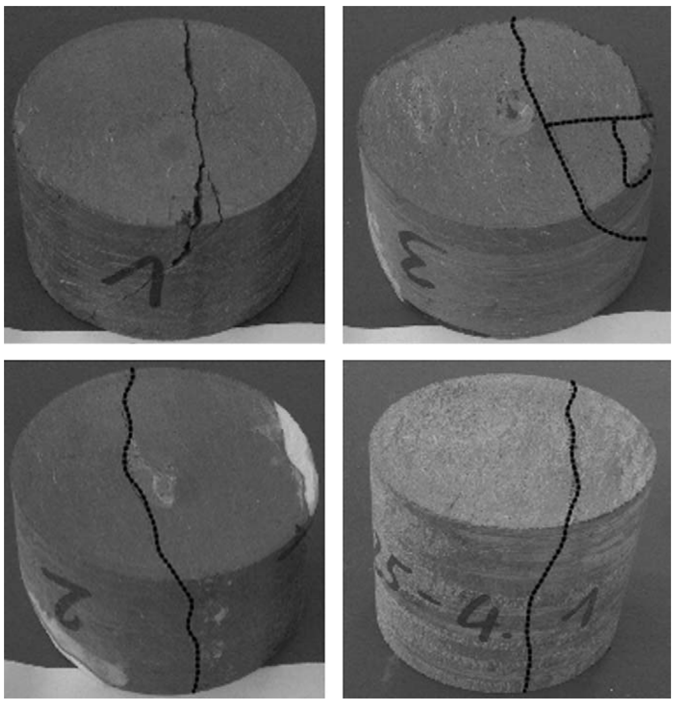

Fig. 9. Examples of generated cracks.

of the samples was between 1.4% and 3.1%. In the framework of earlier laboratory investigations on thermal parameters the initial water content of similar samples from the same borehole was measured between 2.3% and 4.1% [11]. This indicates that even the samples were well coated, a slight drying could not be avoided during storage. Together with the total porosity of 6.9–12.6 Vol%, this equals a water saturation of 28–57 Vol%. The corresponding gas permeability was in the range 3.2×10^{-20}–$1.9\times10^{-16}\,m^2$. Compared to others, the gas permeability of sample D25-1.1 is very low ($3.2\times10^{-20}\,m^2$). It was assumed that this is mainly due to the high water saturation (Fig. 7) impeding the gas flow. The saturation of sample D25-4.2 is comparatively low, which is due to a pre-existing damage of the sample. Due to this damage, correct determination of initial permeability and effective porosity was not possible.

3.2. Tensile strength

To generate artificial cracks for permeability measurements all samples were exposed to a uniaxial pressure continuously increasing from 0 MPa up to their individual tensile strength limit and above. When comparing the results of the tensile strength measurements (Fig. 8) a strong variation of the maximum tensile strength is obvious for all the individual test samples. For the Opalinus clay, tensile strength values between 1.09 and 2.49 MPa were obtained.

Possible reasons for these differences could be different pre-existing damage of the samples due to the drilling process or a slightly varying orientation of the application of force relative to the bedding planes. The orientation of the samples was a difficult task since the bedding was only hardly visible after core preparation. Principally, the obtained values correspond very well with the investigation of Mathier et al., who found values between 1.2 and 2.7 MPa [7,12]. After exceeding the tensile strength of a sample, cracks were generated on a more or less distinct crack plane acting as pre-dominant pathways for fluids (Fig. 9).

3.3. Permeability and porosity as a function of confining pressure

After crack generation, the samples were put into a triaxial pressure cell and the permeability and effective porosity were measured as a function of the stepwise increasing confining pressure. The results of the permeability and effective porosity measurements are shown in Figs. 10 and 11.

The characteristics of the permeability graphs were quite similar for all samples. Although starting at a different level of permeability, the permeability reduction for each sample due to stepwise crack closing was about two orders of magnitude at pressures between 0.25 and 3 MPa. A rapid decrease of permeability can be observed up to a confining pressure of about 1.5 MPa followed by a slower decrease up to 3 and 5 MPa. One could assume that the lower decrease is due to matrix compaction rather than to crack closing, but looking at the initial values prior to cracking (Fig. 7), it is obvious that the initial values are not reached at 1.5 MPa except for sample D25-3.3. Thus, it seems as if the crack is not completely closed and that due to a rough crack surface there is still a small remaining space for the gas to go through. The different starting levels of permeability are due to the fact that the initial cracking of the samples could not be controlled so that not all samples were damaged in the same way. The samples had different pre-existing damages and tensile strengths as explained in Section 3.2. For two of the samples, the confining pressure was increased up to 5.5 MPa resulting in a further continuous decrease of the permeability. The measured decrease of permeabilities are in line with results obtained in [13]. The permeability values correspond well with those found in [14]. In this study, the EDZ of drifts in the underground rock laboratory at Mont Terri was investigated and the mean EDZ permeability was between 10^{-15} and $10^{-14}\,m^2$.

For a better comparison of the permeability development, the measurements for each sample were normalized to their start values at 0.25 MPa (Fig. 12). Generally, the permeability decrease for all samples can be described by

$$k/k(0.25\,\text{MPa}) = a\,p^{b} \quad (2)$$

with k=permeability [m^2], p=confining pressure [MPa], and the empirical parameters taking the values a=0.06 and $b=-2.404$. From Fig. 12, a clear distinction between crack closure effects and matrix compaction effects on permeability as discussed above cannot be made.

To check the behaviour of the Opalinus clay not only under increasing pressure but also under decreasing pressure conditions, the permeabilities of the samples D25-1.1 and D25-7.1 were measured at stepwise decreasing pressure from 5.3 down to 3.0 and 0.25 MPa, respectively (Fig. 13). As can be seen in Fig. 13, the reduction of permeability seems to be an irreversible process. Going down from 5.3 to 3 MPa no increase of permeability was observed. It was not until the lowest confining pressure of

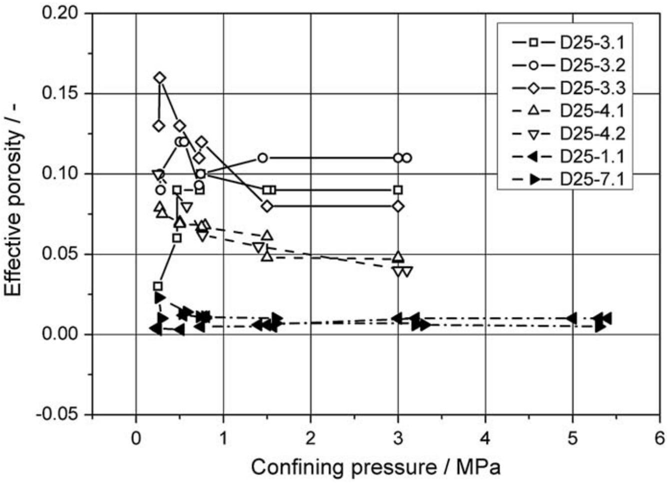

Fig. 11. Effective porosity versus confining pressure.

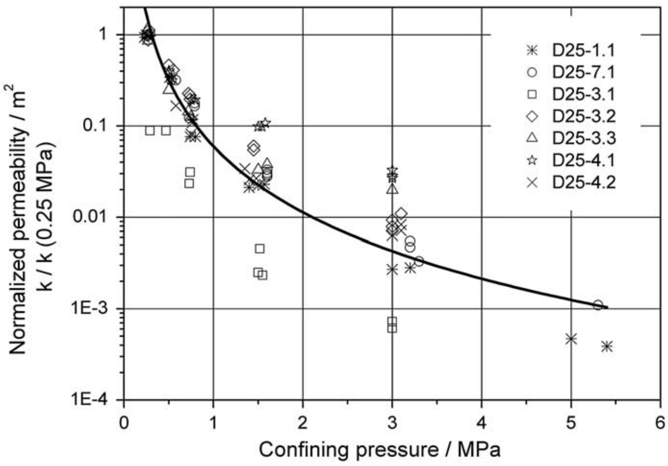

Fig. 12. Permeability reduction versus confining pressure.

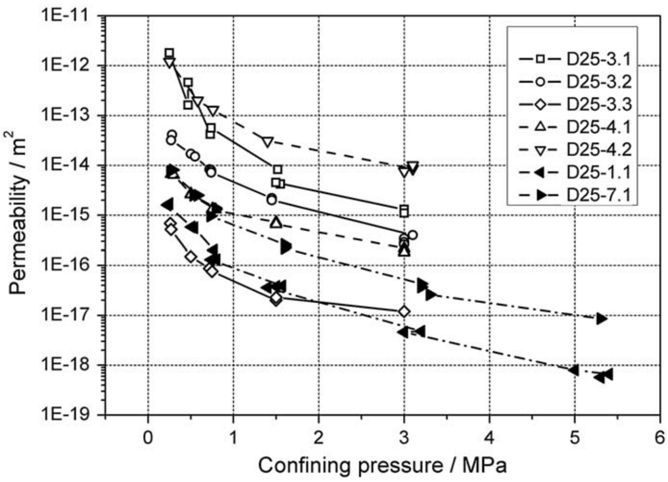

Fig. 10. Permeability versus confining pressure.

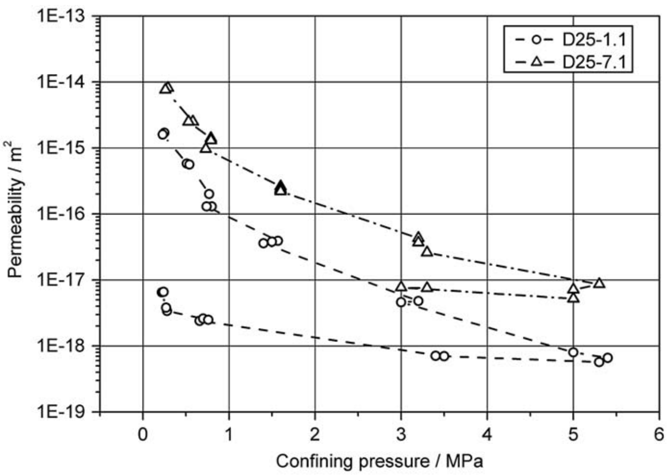

Fig. 13. Permeability versus confining pressure on loading and de-loading path.

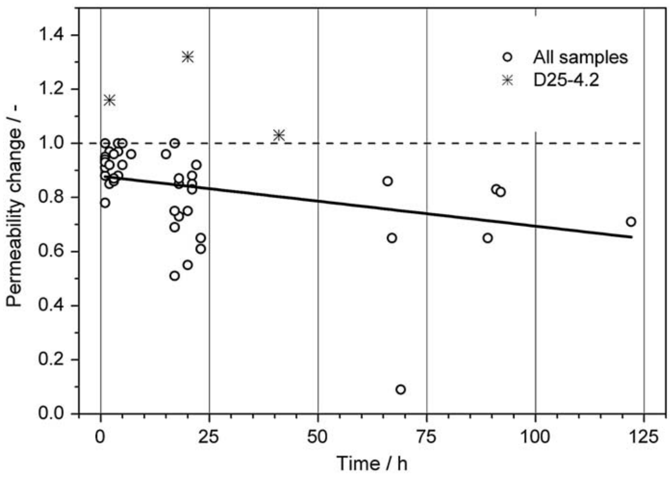

Fig. 14. Permeability versus time at constant pressure.

0.25 MPa was reached that a slight increase in permeability was measured. This led to the assumption that during pressurization some kind of sealing process took place resulting in a permanent crack closure.

Looking at the effective porosity values (Fig. 11) measured during confining pressure increase, the view is a bit different. On the one hand, a distinction can be made between the three different sample types (D25-3.*x*, D25-4.*x*, and D25-*x*.1). For each type, the level of effective porosity is a bit different ranging from about 0.01 for the D25-*x*.1 samples to about 0.1 for the D25-3.*x* ones (Fig. 11). A similar distinction cannot be made by looking at the permeability plot only (Fig. 10). On the other hand, it can be seen that for two samples the effective porosity unexpectedly increased at the beginning of the measurements at low confining pressure. This effect can be interpreted either as a result of an expulsion of water, or as a result of a drying process, since several times a technically dry gas flew through the sample over a longer period of time. Due to the gas flow during the measurement water got out of the sample resulting in a higher effective porosity. At higher pressure steps this effect was not detected any more leading to the assumption that crack closing increased preventing the displacement of any remaining water.

3.4. *Permeability and porosity as a function of time at constant pressure*

The permeability is not only dependent on confining pressure but also on time. At some of the applied pressure levels the permeability of a sample was measured after different periods of time without changing the pressure. Generally, the permeability decreased over time indicating some kind of "creep" behaviour of the Opalinus clay resulting in a slight closure of cracks. To visualize this time dependence, the permeability values obtained for each sample at the different pressure levels were normalized to the first value (Fig. 14). Except for sample D25-4.2, the values obtained at a constant pressure show a decrease of permeability over time. Within a time period of 100 h the permeability reduction is about 30% and it can be assumed that the permeability is reduced even further over longer time periods. The different behaviour of D25-4.2 in this context was assumed to be the result of drying and/or the expulsion of water already explained in Section 3.3. The observed pre-existing fracturing of this sample (see Section 3.1) led to a higher permeability before the permeability was reduced by the compaction process. It can be said that on the one hand the reduction of permeability depends on the reduction of available pore space. On the other hand, the permeability could be further reduced in case of some "creep" behaviour that changes the connectivity of the remaining pore space.

4. Conclusions

The hydraulic properties permeability and effective porosity under increasing and decreasing confining pressure were determined for fissured Opalinus clay samples taken from the Mont Terri underground rock laboratory. As a result, the following conclusions can be drawn:

(i) The initial water content of the samples prior to cracking was between 1.4% and 3.1%. Together with the total porosity of 6.9 to 12.6Vol% this resulted in a water saturation between 28 and 57Vol%.
(ii) The undisturbed gas permeability was between 2.1×10^{-18} and $1.9 \times 10^{-16}\,m^2$, except for sample D25-1.1. Its low gas permeability ($3.2 \times 10^{-20}\,m^2$) was due to the higher water saturation.
(iii) Tensile strength values between 1.09 and 2.49 MPa were obtained. It was assumed that the reason for the differences was due to different pre-existing damage of the samples caused by the drilling process or due to a slightly varying orientation of the application of force relative to the bedding planes.
(iv) A continuous decrease of permeability was determined during increase of confining pressure and a mathematical expression was identified in terms of a potential function that can be used in the framework of a long-term safety analysis. The permeability reduction was roughly two orders of magnitude up to a confining pressure of 3 MPa. In contrast to this, a decrease of confining pressure did not result in an increase of permeability indicating a sealing process of the cracks during pressurization. It should be mentioned that predictive calculation for permeability evolution should take into consideration that the observed permeability reduction is valid only for the investigated pressure range.

The obtained results of the laboratory investigations yielded an increased understanding of the pressure and time-dependent permeability behaviour of fissured Opalinus clay samples. Prior to a transfer of these results to real EDZ behaviour a verification by an in-situ test is necessary.

Acknowledgements

We thank the Federal Ministry of Economics and Technology (BMWi: Bundesministerium für Wirtschaft und Technologie) for funding the research and development activities described in this report under Contract no. FKZ 02E10086.

References

[1] Jobmann M, Amelung P, Uhlig L. Untersuchungen zur sicherheitstechnischen Auslegung eines generischen Endlagers im Tonstein in Deutschland, GENESIS, Abschlussbericht, DBE Technology, Peine; 2007.
[2] Jobmann M, Uhlig L, Amelung P, Schmidt H, Polster M, Billaux D, Hoth P. Investigations on safety relevant repository design in German clay formations. In: Proceedings of international conference on clays in natural and engineered barriers for radioactive waste confinement, Lille, France, 2007.
[3] Blümling P, Bernier F, Lebon P, Martin D. The excavation damaged zone in clay formations, time-dependent behaviour and influence on performance assessment. Phys Chem Earth 2007;32:588–99.
[4] Buehler Ch, Heitz D, Trick Th, Frieg B. In-situ self-healing of the EDZ as a consequence of loading. Impact of the excavation disturbed or damaged zone (EDZ) on the performance of radioactive waste geological repositories.

In: Proceedings of a European commission CLUSTER conference, Luxemburg, 2003, p. 231–236.
[5] Bastiaens W, Bernier F, Li XL. SELFRAC: Experiments and conclusions on fracturing, self-healing and self-sealing processes in clays. Phys Chem Earth 2007;32:600–15.
[6] Davy CA, Skoczylas F, Barnichon JD, Lebon P. Permeability of macro-cracked argillite under confinement: gas and water testing. Phys Chem Earth 2007;32:667–80.
[7] Nationale Gesellschaft für die Lagerung radioaktiver Abfälle (NAGRA). Technischer Bericht 02-03. Projekt Opalinuston, Synthese der geowissenschaftlichen Untersuchungsergebnisse, Wettingen, Schweiz, 2002.
[8] Jobmann M, Amelung P, Engelhardt HJ, Uhlig L. Auswirkung einer Temperaturerhöhung auf die Auslegung geotechnischer Barrieren, die Stabilität von Einlagerungsbohrlöchern und die Materialeigenschaften von Tonsteinformationen, Projektträger Forschungszentrum Karlsruhe, Statusbericht, Karlsruhe, 2008.
[9] DGED. Indirekter Zugversuch an Gesteinsproben—Spaltzugversuch. Techn. Prüfvorschriften für Boden und Fels im Straßenbau TP BF-StB, Teil C10, Deutsche Gesellschaft für Erd- und Grundbau, Empfehlung Nr. 10, Ausgabe 1985.
[10] Häfner F, Kornjaew A, Pohl A, Voigt HD. Permeabilitäts—und Porositätsmessungen an Gesteinsproben mit dem instationären Zweikammerverfahren. Erdöl Erdgas Kohle 1996;112(10):401–4.
[11] Buntebarth G. Bestimmung der Wärmeleitfähigkeit von Tonsteinproben, Internal Report, DBE TECHNOLOGY, Peine, 2004 (unpublished).
[12] Mathier JF, Egger P, Descoeudres F. Sondierbohrung Benken. Felsmechanische Untersuchungen an Bohrkernen (Teil 2), Nagra Internal Report, 1999 (unpublished).
[13] Zhang CL, Rothfuch T, Dittrich J, Müller J. Investigations on self-sealing of indurated clay, part of the NF-PRO project, Final Report, GRS-230, ISBN 978-3-939355-04-5, Braunschweig, Germany, 2008.
[14] Bossart P, Trick Th, Meier PM, Mayor JC. Structural and hydrogeological characterisation of the excavation-disturbed zone in the Opalinus Clay (Mont Terri Project, Switzerland). Appl Clay Sci 2004;26:429–48.